Reports

The Microstructure of High–Critical Current Superconducting Films

P. CHAUDHARI, F. K. LEGOUES, ARMIN SEGMÜLLER

The microstructure of superconducting films that have shown high–critical current densities has been studied. The films are shown to be epitaxial and contain twins and precipitates. The main difference between these films and low current carrying samples is the absence of grain boundaries. These boundaries are therefore identified as the cause of the lower critical current in ceramic samples.

THE PRACTICAL USE OF SUPERCONducting materials requires (i) a high transition temperature, (ii) a large critical current, and (iii) the ability to fabricate superconducting materials into forms useful for applications. Bednorz and Müller (*1*) have shown that the copper oxide–based structures have high superconducting transition temperatures. Since their work, a number of groups have independently obtained superconducting materials with transition temperatures above 90 K (*2*). The second requirement was demonstrated by Chaudhari *et al.* (*3*), who showed that critical currents in excess of 10^5 A cm^{-2} could be obtained at liquid nitrogen temperature (77 K) in the high-temperature superconductors. A large number of groups are currently exploring the fabrication of these materials into films, tapes, and wires. In this report we describe the microstructure of the materials used to obtain high critical currents.

The films were deposited on strontium titanate substrates by evaporation from three electron-beam sources. The three metallic elements (yttrium, barium, and copper) were deposited in an oxygen pressure of approximately 10^{-4} torr; the substrate was heated to 400°C during deposition. Subsequent to the evaporation the films were flash-heated for 1 second at 950°C in air followed by a heat treatment in flowing oxygen at approximately 900°C as previously described (*3*). The composition of the films was chosen to have excess yttrium and copper relative to the barium. We hoped that this would provide oxide precipitates that would impede vortex motion and also compensate for any strontium diffusion from the substrate into the film during the annealing of the film. Films produced this way were examined by x-ray diffraction and transmission electron microscopy.

IBM Thomas J. Watson Research Center, Yorktown Heights, NY 10598.

The x-ray data were obtained with Cu-Kα radiation by means of a conventional x-ray diffractometer with a grooved germanium crystal monochromator for high resolution and a grazing-incidence x-ray diffractometer with somewhat lower resolution (*4*). The diffraction pattern shown in Fig. 1 was obtained in a θ-2θ scan (where θ is the Bragg angle) on the conventional diffractometer. In this geometry, where the diffraction vector is perpendicular to the plane of the film, we see only the multiple-order reflections (00ℓ) that indicate a preferred orientation or texture with the *c*-axis perpendicular to the plane of the film. An x-ray pole-figure analysis showed that the film was not just textured with a fiber axis but was aligned with the single-crystal substrate in a true epitaxy. To quantify the degree of epitaxial alignment the films were also characterized by grazing-incidence diffraction in a geometry in which the diffraction vector is parallel to the plane of the film. The diffraction pattern shown in Fig. 2 was obtained in a θ-2θ scan through the orthorhombic (020) and (200) reflections. The appearance of both reflections in one θ-2θ scan proves that the epitaxial film consists of two domains that are rotated 90° around the *c*-axis. A θ-2θ scan through the {110} reflections showed only one well-defined line since the (110) and the ($\bar{1}$10) reflections are equivalent in orthorhombic crystals. In ω scans, that is, with the detector fixed at the Bragg angle 2θ and the sample rotated around the normal of the film plane, we found that the orientational spread of the (020) and (200) planes was only slightly larger than that of the cubic substrate's (200) planes. However, the (110) film plane had a somewhat larger orientational spread because the (110) planes in the two domains are not parallel but enclose an angle of 0.83°. The lattice parameters deduced from the x-ray data were a = 3.832 Å (5), b = 3.888 Å (5), and c = 11.753 Å (4), with the probable error of the last digit in parentheses. In addition to the diffraction lines from the bulk of the film we also observed relatively weak lines associated with the presence of yttrium and copper oxides.

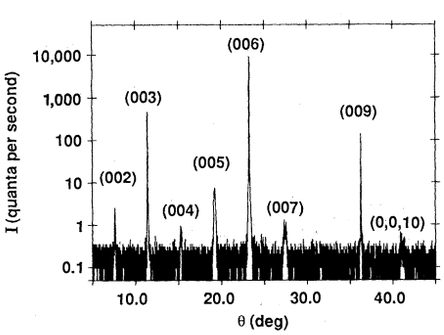

Fig. 1. X-ray diffraction intensity I versus angle for a θ-2θ scan of the superconducting film.

In addition to x-ray diffraction, we examined the films with a transmission electron microscope. The samples were mechanically ground to about 50 μm and then ion-milled to electron transparency. Both plane view and cross-sectional samples were prepared. The flat-on samples (plane view) were prepared so that the layer of superconducting material closest to the interface could be observed. This was done by ion-milling the sample on the film side for very short periods of time at the end of the sample preparation process. This was necessary since the heat treatment had been designed to obtain nucleation of the superconducting phase both at the substrate and the free surface. The film was expected to be epitaxial near the substrate interface and to have different crystallographic orientation near the surface. We believed that the top layer would help pin vortices down as a result of the anisotropic nature of these materials. Figure 3 shows a lattice image of the interface obtained from a cross-sectional sample. The orientation and registry between the substrate and the superconducting films are clearly visible. The interface is nearly atomically flat and no

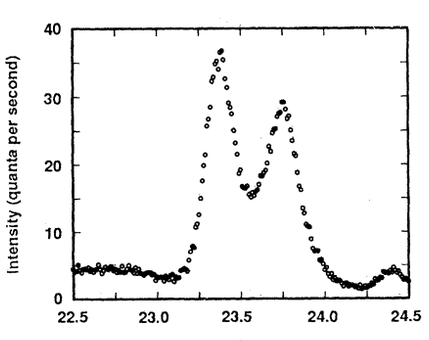

Fig. 2. X-ray diffraction intensity versus angle for a θ-2θ scan through the orthorhombic (020) and (200) reflections.

other phase or compound is visible. This establishes the presence of epitaxy. In Fig. 4 we show a plane-view micrograph in which yttrium oxide precipitates are visible. These were present throughout the film. Fewer and much coarser copper oxide precipitates were also present. The exact composition of the precipitates was deduced both from energy-dispersive x-ray measurements and from the diffraction pattern in the electron microscope. The copper oxide precipitates have a definite orientation with respect to the superconducting film whereas the yttrium oxide precipitates are randomly oriented (see inset diffraction pattern, Fig. 4). This, as well as the fact that no yttrium oxide is at equilibrium with the superconducting phase at the annealing temperature, indicates that it probably forms before annealing. By contrast, copper oxide precipitates out during annealing, thus explaining the orientation relation. The presence of numerous twins in the superconducting phase shows that it is indeed orthorhombic (since the twins are equivalent to switching the *a*- and *b*-axes) and that the two domains rotated 90° around the *c*-axis, described earlier, are closely intermixed.

The structure of these films was designed to optimize vortex pinning and, at the same time, to minimize the occurrence of the structure of the type observed in pressed samples or evaporated polycrystalline films. In the latter, grain boundaries and voids are expected to be detrimental. In order to test this hypothesis we also prepared polycrystalline films. The micrograph in Fig. 5 was obtained from such a film. It shows many of the defects observed in the epitaxial films along with grain boundaries. The important difference between the film shown in Fig. 5 and the film shown in Fig. 4 is the former's inability to carry large currents.

In typical metallic systems grain boundaries are abrupt, with a transition thickness equal to approximately one atomic layer. In contrast, in substances in which the unit cell is large we expect the transitional thickness to be larger than the geometrical width obtained from simple packing when the atoms are simulated by hard spheres. In the particular case of the orthorhombic unit cell of these superconductors, we expect the grain boundaries to be wide. Grain boundaries can usually be described in terms of lattice dislocations. The Burgers vector of the latter usually meshes with the underlying lattice. In the case of the *c*-axis of this orthorhombic structure the unit cell is large, 11.753 Å, and, as the energy of the dislocation is proportional to the square of the Burgers vector, it is unlikely that a simple dislocation can exist. If superdislocations rather than simple dislocations are present, the width of the boundary is still likely to be determined by the spacing between dislocations comprising the superdislocation. In either case, dislocation theory would predict that the boundary width will be large. In this regard, highly textured films, with the *c*-axis perpendicular to the substrate but randomly oriented in the plane, may have different properties than completely random films because the grain boundaries will be narrower as the lattice parameters in this orientation are smaller. Coincidentally, the coherence length is also larger for this orientation. Both of these factors favor stronger superconducting coupling and therefore a larger critical current. Finally, it is interesting to note that, in addition to second-phase precipitate, twinning is copiously present in the epitaxial films and may be responsible for the strong pinning deduced from critical

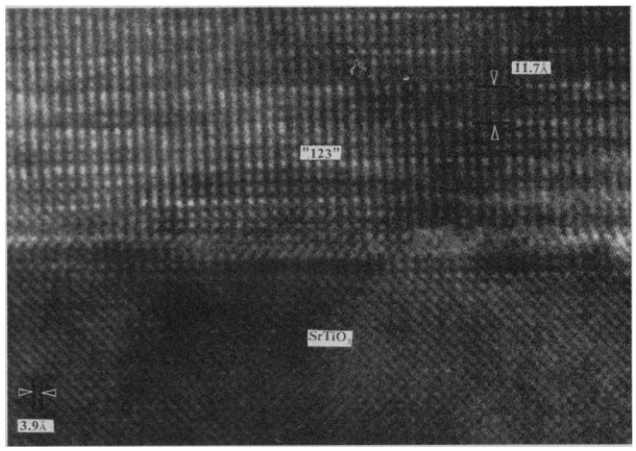

Fig. 3. High-resolution lattice image of the superconductor ("123")/substrate interface.

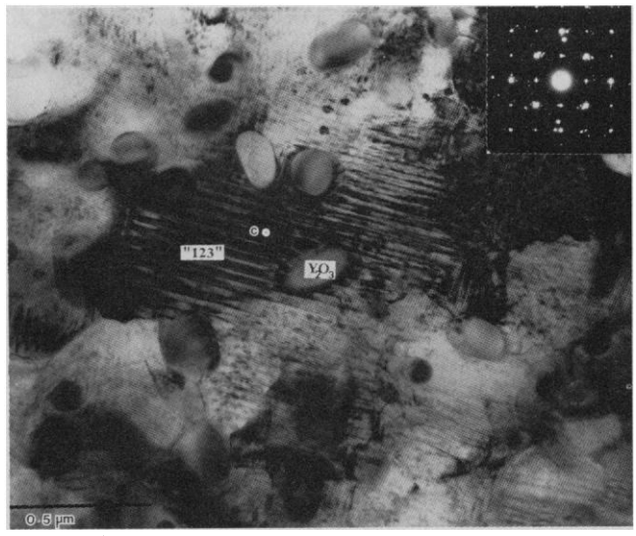

Fig. 4. Plane-view micrograph of the superconducting film. The *c*-axis is perpendicular to the plane of the figure. Inset shows electron diffraction pattern.

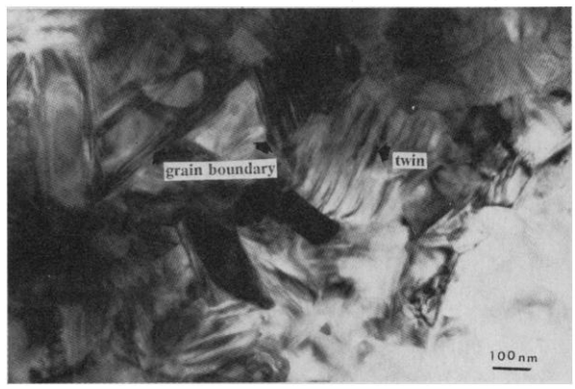

Fig. 5. Plane-view micrograph of a nonepitaxial superconducting film showing approximately the same superconducting transition temperature as the epitaxial film but a much lower critical current density. Note the presence of grain boundaries and twins.

current measurements. However, because of the crystallographic dependence of the twin planes, such pinning must also be anisotropic.

REFERENCES AND NOTES

1. J. G. Bednorz and K. A. Müller, *Z. Phys.* **B64**, 198 (1986).
2. M. K. Wu *et al.*, *Phys. Rev. Lett.* **58**, 908 (1987); Z. Zhao *et al.*, *Kexue Tongbao*, in press; S. Hikami, T. Hirai, S. Kagashima, *Jpn. J. Appl. Phys.* **26**, L314 (1987).
3. P. Chaudhari, R. H. Koch, R. B. Laibowitz, T. R. McGuire, R. J. Gambino, *ibid.*, p. 2684.
4. A. Segmüller, *Adv. X-Ray Anal.* **29**, 353 (1986).

17 July 1987; accepted 9 September 1987

Downregulation of L3T4$^+$ Cytotoxic T Lymphocytes by Interleukin-2

CHARLES C-Y. SHIH AND ROBERT L. TRUITT

Proliferation of activated cytotoxic T lymphocytes (CTLs) that recognize foreign histocompatibility antigens is induced by interleukin-2, a potent immunoregulatory molecule originally described as T cell growth factor. Interleukin-2 (IL-2) is widely used to isolate and induce clonal expansion of CTLs for functional studies in vitro and in vivo. However, in studies with CTLs specific for class I and class II histocompatibility antigens, IL-2 rapidly downregulated the lytic activity of some class II–specific CTLs in a time- and dose-dependent manner. Lytic activity of L3T4$^+$ CTLs specific for the murine class II antigen I-E^k was repeatedly up- and downregulated in vitro by alternate exposure to specific (alloantigen) and nonspecific (recombinant IL-2) signals, respectively. These results demonstrate that some CTLs modulate their functional property (cytolysis) while undergoing IL-2–driven cell proliferation without loss of antigen specificity or ability to revert to a lytic phenotype.

INTERLEUKIN-2 (IL-2) IS A SOLUBLE glycoprotein that causes cell proliferation when it binds to cells via a specific membrane receptor (*1–3*). Various immunoenhancing activities have been ascribed to IL-2 (*2–5*), including clonal expansion of activated cytotoxic T lymphocytes (CTLs) directed against alloantigens encoded by the major histocompatibility complex (MHC). We now report that IL-2 can also rapidly downregulate, in a dose-dependent manner, the lytic activity of at least some class II antigen–specific CTLs without affecting their ability to undergo antigen-driven proliferation in the absence of IL-2. Downregulation of lytic activity occurred when murine CTLs specific for the MHC molecule encoded by I-E^k were exposed to IL-2 for at least 6 hours. These class II antigen–specific CTLs could be repeatedly induced to gain and lose lytic function in a cyclical fashion by alternate exposure to specific (alloantigen) and nonspecific (IL-2) environmental signals.

The CTL cell line used in these studies is designated SATC. SATC cells were derived from the wells of a limiting-dilution microcytotoxicity assay (*6*) in which the responder cells were splenocytes obtained from an allogeneic bone marrow chimera (SJL → AKR) that had been given SJL (H-2^s) bone marrow cells together with a noncytotoxic class II antigen–specific SJL T cell clone designated SAC-9.12 [see (*7*) for description of clone] 4 weeks earlier. After 7 days of coculture with irradiated AKR (H-2^k) stimulator cells in the presence of IL-2–conditioned medium obtained from a secondary mixed leukocyte culture, a portion of the cells from each well were tested for cytotoxicity against E8/AK.D1, a leukemic AKR cell line. The cells taken from several cytolytic microwells were subsequently pooled and maintained thereafter in culture wells (35 mm) or tissue culture flasks (25 cm^2) containing complete Dulbecco's modified Eagles medium (C-DMEM) (*6*) plus recombinant IL-2 (rIL-2) at 2.5 U/ml [*Escherichia coli*–derived human IL-2 (Ala-125); Amgen Biologicals, Thousand Oaks, California] without further antigen stimulation. Cell cultures were split every 3 or 4 days to attain a concentration of 1×10^5 cells per milliliter. Clones and subclones were established from the parent SATC culture by standard limiting-dilution techniques (*8*).

Flow cytometric analysis (*9*) showed the original SATC cells to be T lymphocytes of SJL (Thy-1.2) and not AKR (Thy-1.1) origin. More than 99% of the cells were Thy-1.2$^+$, L3T4$^+$, Ly-1$^-$, and Ly-2$^-$. All clones and subclones isolated from the SATC line had the same cell-surface phenotype as the parent line.

Department of Pediatrics, Medical College of Wisconsin, Children's Hospital of Wisconsin, Milwaukee, WI 53233.

SATC cells showed rIL-2–driven cell proliferation in the absence of alloantigen (Table 1). In addition, they proliferated in the absence of rIL-2 when stimulated with cells that expressed I-E^k–encoded MHC molecules [for example, cells from B10.BR, B10.A, and B10.A(5R), but not B10.A(4R) mice] (Table 1). The response of SATC clones and subclones was identical to that of the parent line (*9*).

SATC cells were found to be highly cytolytic for H-2^k targets when tested in the original limiting-dilution microcytotoxicity assay immediately after isolation from the SJL → AKR chimera, but they were not lytic when retested in standard 3.5-hour cell-mediated lympholysis (CML) assays after 2 weeks of continuous culture in rIL-2. However, SATC cells obtained from antigen-driven proliferation assays (in which the rIL-2 had been removed 72 hours earlier) reexpressed cytolytic activity (Table 1). Their lytic activity was directed specifically against I-E^k–bearing target cells.

The absence of lysis by SATC cells cultured in rIL-2 suggested to us that IL-2 may have downregulated lytic activity. To test this, we washed SATC cells free of rIL-2–supplemented maintenance medium and recultured them for 2 to 72 hours in medium alone, medium plus rIL-2, or medium plus alloantigen (no added IL-2) (Fig. 1A). In cultures containing rIL-2, no significant lysis was observed at any of the times tested. In contrast, cytolytic activity reappeared be-

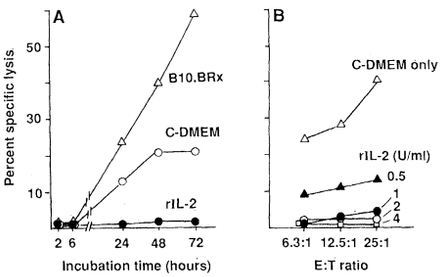

Fig. 1. (**A**) Nonlytic SATC cells were washed free of rIL-2 maintenance medium and placed in multiple culture wells (35 mm) containing 2×10^6 SATC cells per 8 ml of C-DMEM plus rIL-2 (4 U/ml) (●), 5×10^6 cells per 8 ml of C-DMEM alone (○), or 5×10^6 cells per 8 ml of C-DMEM plus 20×10^6 BRx cells per well (△). After incubation for the times indicated, effector cells were collected, washed, and tested in CML assays (see Table 1) with E8/AK.D1 target cells. Data are shown as percent specific lysis at an E:T ratio of 25:1 for each time point. (**B**) SATC cells (5×10^6) were washed free of rIL-2 and cocultured with BRx stimulator cells (20×10^6) in 8 ml of C-DMEM alone (△) or C-DMEM supplemented with rIL-2 at a final concentration of 0.5 (▲), 1.0 (●), 2.0 (○), or 4.0 (□) U/ml. After 72 hours of culture, CML assays were done at the E:T ratios shown with E8/AK.D1 target cells. Representative results from one of three replicate experiments are shown.